



The Influence of Overlapping Band Filters on Octave Band Decay Curves

Marbjerg, Gerd; Brunskog, Jonas; Jeong, Cheol-Ho; Zapata Rodriguez, Valentina

Published in:
Acta Acustica United with Acustica

Link to article, DOI:
[10.3813/AAA.919259](https://doi.org/10.3813/AAA.919259)

Publication date:
2018

Document Version
Publisher's PDF, also known as Version of record

[Link back to DTU Orbit](#)

Citation (APA):
Marbjerg, G., Brunskog, J., Jeong, C.-H., & Zapata Rodriguez, V. (2018). The Influence of Overlapping Band Filters on Octave Band Decay Curves. *Acta Acustica United with Acustica*, 104, 943 – 946.
<https://doi.org/10.3813/AAA.919259>

General rights

Copyright and moral rights for the publications made accessible in the public portal are retained by the authors and/or other copyright owners and it is a condition of accessing publications that users recognise and abide by the legal requirements associated with these rights.

- Users may download and print one copy of any publication from the public portal for the purpose of private study or research.
- You may not further distribute the material or use it for any profit-making activity or commercial gain
- You may freely distribute the URL identifying the publication in the public portal

If you believe that this document breaches copyright please contact us providing details, and we will remove access to the work immediately and investigate your claim.

The Influence of Overlapping Band Filters on Octave Band Decay Curves

Gerd Marbjerg¹⁾, Jonas Brunskog¹⁾, Cheol-Ho Jeong¹⁾, Valentina Zapata-Rodriguez^{2,1)}

¹⁾ Acoustic Technology, Department of Electrical Engineering, Technical University of Denmark, 2800 Kgs. Lyngby, Denmark. jbr@elektro.dtu.dk

²⁾ Interacoustics Research Unit, 2800 Kgs. Lyngby, Denmark

Summary

This study showed that the overlap of practically-used bandpass filters can influence the octave band decay curves, especially if the decays are calculated from a filtered impulse response that has been created from octave band energy responses. Energy from a frequency band with a long reverberation time can leak into a neighbouring band with a shorter reverberation time. This also means that neither octave band decays from a measured response are independent, nor are measured octave band reverberation times.

© 2018 The Author(s). Published by S. Hirzel Verlag · EAA. This is an open access article under the terms of the Creative Commons Attribution (CC BY 4.0) license (<https://creativecommons.org/licenses/by/4.0/>).

1. Introduction

When using energy-based geometrical room acoustic modelling techniques, room acoustical parameters are normally calculated at the centre frequency of octave bands. This assumes that the energy response in each band only depends on the material properties of the very band. If these results are to be used for auralisations, it is necessary to create a total full bandwidth pressure impulse response from the octave band energy impulse responses [1, 2, 3, 4]. Here, full bandwidth response refers to a response that covers the entire frequency range of interest, typically the audible range. The full bandwidth pressure response can be obtained by first creating octave band pressure impulse responses and then summing these.

If the full bandwidth pressure impulse response is re-filtered into octave band impulse responses, the decays of these are unlikely to be the same as the decays of the responses from before the summation, because of overlaps between adjacent bands that cause energy leakage. Reverberation times are often calculated from the octave band responses, expecting these to be valid also for the full bandwidth impulse response. This letter demonstrates that they are not necessarily so. When measured impulse responses are processed with bandpass filters, the decays in the bands are not independent, and simulations assuming independent bands therefore do not correspond to measurements.

This study focuses on decay curves and reverberation times, because the effect of the frequency leakage is much

larger when considering the energy decay than the total energy or the steady state response.

The phenomenon is not limited to energy-based models, because one might use a pressure-based model to calculate an impulse response within a octave band and determine the decay from this. In this case, it is also possible that the obtained decay will not correspond to one that would be obtained if the impulse response of a wider frequency range had been calculated and then filtered to the octave band.

To the best knowledge of the authors, this issue of overlapping bands has not yet been sufficiently discussed in this application field. A related issue for measurements of narrow band decays, is the influence of the time responses of the filters, which has been studied [5, 6]. The present study illustrates how the overlapping bands influences the decays from energy-based models, and investigates this through simple examples.

2. Full bandwidth impulse response

A full bandwidth impulse response from energy-based methods is often found by first determining octave band impulse responses and then taking the sum of those as

$$p(t) = \sum_b p_b(t), \quad (1)$$

where $p_b(t)$ is the impulse response of the octave band b . $p_b(t)$ can for instance be found with an octave band noise signal that is used to fill an energy impulse response. The octave band impulse response will in that case be given by

$$p_{b,noise}(t) = (n(t) * h_b(t)) \sqrt{w_b(t)}, \quad (2)$$

Received 23 March 2018,
accepted 1 September 2018,
published online 10 October 2018.

where $w_b(t)$ is the energy impulse response of the band b , $n(t)$ is a Gaussian noise signal, and $h_b(t)$ is the impulse response of the filter of band b . $n(t) * h_b(t)$ is thus a octave band noise signal of which the content will be mainly within the cutoff frequencies of the band b , but there will be some content outside depending on the sharpness of the filter. The method of Equation (2) is, for example, used to obtain a pressure impulse response from acoustical radiosity in the simulation tool PARISM [4]. A Poisson process with random sign can also be used rather than the Gaussian noise signal [3].

To compare with Equation (2), a method that does not employ bandpass filters is tested. The rationale behind this approach is to limit the overlaps of the octave band responses. For this, sine functions of random phases are used, and the impulse response within a single band is then given by

$$p_{b,\sin}(t) = \sum_{l=1}^L \sin(2\pi f_l t + \varphi_l) \sqrt{w_b(t)}, \quad (3)$$

where L is the number of included sines within band b and φ_l is a random phase. f_l refers to frequencies between the lower and upper cutoff frequencies of band b . With this formulation, the overlap of the bands in the creation of the full bandwidth response only comes from the attenuation of the sines due to the decay factor $\sqrt{w_b(t)}$.

Regardless of whether $p_{b,\text{noise}}$ or $p_{b,\sin}$ is used, there will be an overlap of the bands if the full bandwidth response is refiltered with non-ideal filters. By comparing $p_{b,\text{noise}}$ and $p_{b,\sin}$, it can be determined how much of the total effect is due to the fact the filters in $p_{b,\text{noise}}$ overlap, and how much is due to the overlap of the filters for refiltering. The refiltered octave band response is found as

$$p_{b,RF}(t) = p(t) * h_b(t), \quad (4)$$

where the subscript RF denotes that it is the refiltered response, and $p(t)$ is found with Equation (1). In the following $p_{b,\text{noise},RF}$ refers to a $p_{b,RF}$ using $p_{b,\text{noise}}$ in Equation (1), and $p_{b,\sin,RF}$ refers to a $p_{b,RF}$ using $p_{b,\sin}$ in Equation (1).

3. Example with geometrical room acoustics

Firstly, the influence of overlapping bands on decay curves is illustrated with an example using the room acoustical simulation tool CARISM [7] (Combined Acoustical Radiosity – Image Source Method). CARISM is an energy-based combination of acoustical radiosity (AR) and the image source method (ISM), and the results from CARISM are octave band energy impulse responses. The method of Equation (2) is applied to obtain a pressure impulse response, and the filters used there and in the refiltering are octave bandpass filters constructed from the 7th order high- and low-pass Butterworth filters. The bandpass filters are constructed such that the sum of their frequency

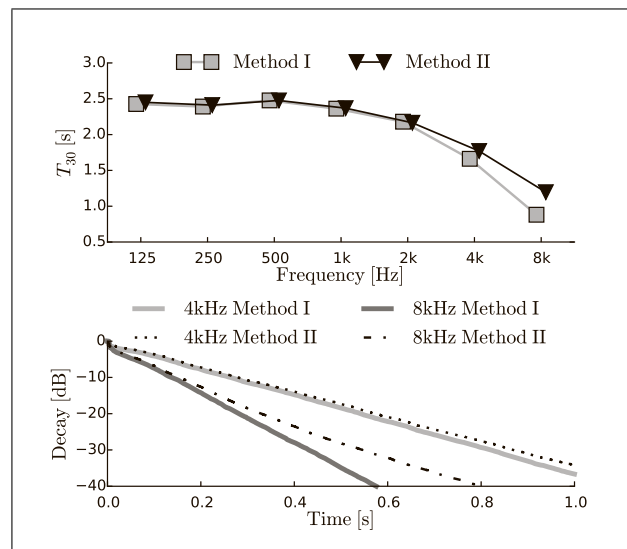


Figure 1. Reverberation times T_{30} (above) and decay curves (below) from a CARISM simulation.

responses is flat, and they meet the requirements of IEC 61260-1 [8].

Octave band decay curves and reverberation times from CARISM can then be obtained with two methods. **Method I:** Directly from the octave band energy impulse responses ($w_b(t)$), where the octave band results are independent of each other. This is the standard method in CARISM. **Method II:** By filtering the full bandwidth impulse response that is constructed, Equation (4).

The chosen test room is based on an existing room at the laboratories of the Technical University of Denmark and has dimensions $[4.38 \times 3.29 \times 2.7]$ m. The calculations are done in the octave bands from 125 Hz to 8 kHz, and the sampling frequency for the pressure impulse response is 24 kHz. The scattering coefficients of all surfaces are set to $[0.03, 0.04, 0.05, 0.06, 0.07, 0.08, 0.09, 0.1]$ for the eight octave bands, respectively. The absorption coefficient is 0.05 for all surfaces and frequencies. The air absorption is determined according to ISO 9631-1 [9], and since the surface absorption is frequency-independent most of the differences in reverberation times over frequency will be due to the air absorption. The reverberation times T_{30} , calculated with both methods I and II, are plotted in Figure 1. Differences are seen between the two methods at 4 and 8 kHz, and that values obtained with method II are higher than those of method I to II.

The decay curves for the 4 kHz and 8 kHz bands from methods I and II are plotted in the lower part of Figure 1. The 8 kHz curve of method II follows the 8 kHz method I curve in the very early part, and then the slope changes to be more similar to that of the 4 kHz method I curve. This indicates that energy from the 4 kHz band is influencing the 8 kHz band in the part of the decay where the energy is low in the 8 kHz band. It is also observed that the curve of 8 kHz band of method II is tending more towards being double-sloped than that of method I. The 4 kHz curves of the two methods are more similar.

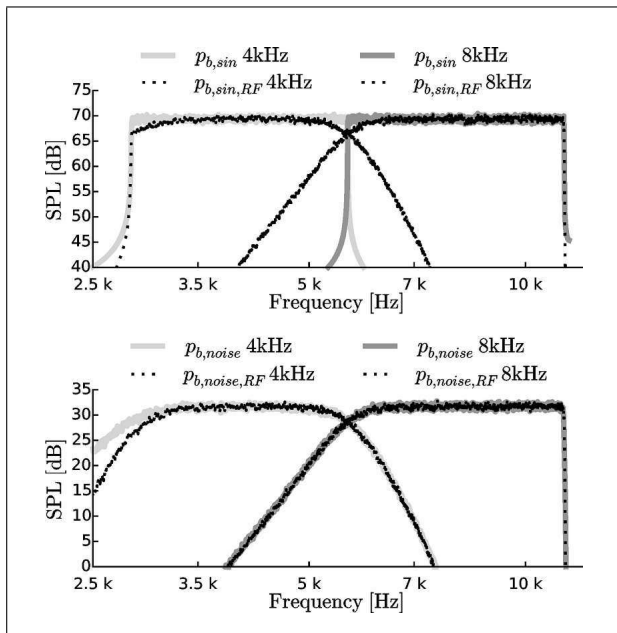


Figure 2. Frequency responses.

4. Examples with exponential decays

The energy impulse responses of Eqs. (2) and (3) are then chosen to decay exponentially. We thus set $\sqrt{w_b(t)} := e^{-\delta_b t}$, rather than determining $w_b(t)$ through a simulation as in Section 3. δ_b is the exponential decay constant, from which the reverberation time can be found by $T = 3 \ln(10)/\delta$. The initial filters used here are the same as in the example of Figure 1.

As in the previous example, the 4 kHz and 8 kHz octave bands are used. Firstly, the frequency responses of the two bands are regarded with both reverberation times set to 0.9 s. The spacing of the frequencies f_i in Equation (3) is 1 Hz. The realisations of $p_{b,noise}$ and $p_{b,sin}$ were repeated 200 times, because each realisation will be slightly different due to the random noise in $p_{b,noise}$ and the random phases in $p_{b,sin}$. The frequency responses are calculated by the Fourier transform of the impulse responses and the means of the squared magnitudes of the 200 realisations of frequency responses are plotted in Figure 2. The overlap of the $p_{b,sin}$ frequency responses is very small (0.085% of the total energy), which makes good sense. The overlap of the frequency responses of $p_{b,sin,RF}$ is then much larger (4.3% of the total energy). The frequency responses of $p_{b,noise}$ overlap much already, so it is barely increased for $p_{b,noise,RF}$ (from 4.3% to 4.4% of the total energy).

A difference in the reverberation times between the 4 kHz and 8 kHz octave bands is then introduced. They are set to 1.7 and 0.9 s, respectively, which are taken from the example of Figure 1.

The mean decay curves from 200 realisations of $p_{b,noise}$ and $p_{b,noise,RF}$ are shown in Figure 3. $p_{b,sin}$ and $p_{b,sin,RF}$ are left out of this figure because they are very similar. The decay curve of $p_{b,noise,RF}$ in the 8 kHz band is very much influenced by the 4 kHz band. It is not single-sloped and

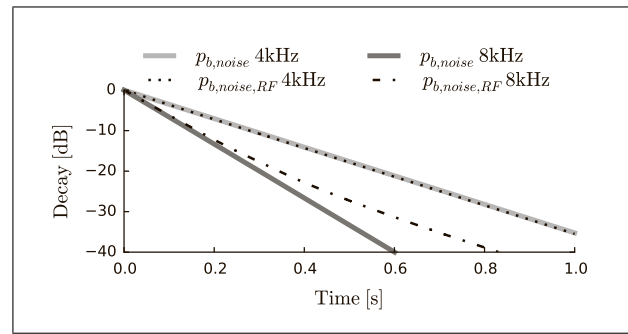


Figure 3. Decay curves.

Table I. Percentage differences in T_{30} and EDT from p_b to $p_{b,RF}$. Note that the JND is 5%.

	7th order filters		9th order filters	
	4 kHz	8 kHz	4 kHz	8 kHz
$\Delta T_{30,p_{b,noise}}$	-0.19%	38%	-0.15%	32%
$\Delta T_{30,p_{b,sin}}$	-0.13%	29%	-0.10%	23%
$\Delta EDT_{p_{b,noise}}$	-2.00%	7.3%	-1.50%	5.6%
$\Delta EDT_{p_{b,sin}}$	-1.31%	3.0%	-1.01%	3.9%

follows the one of 8 kHz p_b for the very first part of the decay, but in the later part the slope approaches that of the 4 kHz $p_{b,noise}$ decay. The $p_{b,noise}$ and $p_{b,noise,RF}$ decays for the 4 kHz band coincide, which confirms that the leakage between bands mostly influences the band with the shorter reverberation time.

The mean reverberation time (T_{30}) and mean early decay time (EDT) of the 200 realisations were also calculated, and the relative differences between those from $p_{b,noise,RF}$ and $p_{b,sin,RF}$, and those from $p_{b,sin}$ and $p_{b,noise}$ are calculated as

$$\Delta T_{30,p_b} = (T_{30,p_{b,RF}} - T_{30,p_b}) / T_{30,p_b} \cdot 100\% \quad (5)$$

$$\Delta EDT_{p_b} = (EDT_{p_{b,RF}} - EDT_{p_b}) / EDT_{p_b} \cdot 100\%,$$

where the T_{30} and EDT values are means of the 200 realisations. In Table I, it is seen that the difference is obviously largest for the 8 kHz band, and that it is the reverberation time that is most influenced. For the 8 kHz bands, the changes in reverberation times are above the just noticeable difference, which is stated as 5% in ISO 3382-1 [10]. For the 8 kHz early decay times, it is only $\Delta EDT_{p_{b,sin}}$ that is below the just noticeable difference. For the 4 kHz values there are also small changes, all below the just noticeable difference. But since the differences are consistently reductions, they cannot be random and must stem from the leakage. The changes are generally smaller for $p_{b,sin,RF}$, but still large enough to show that the overlap of the refiltering filters can create a noticeable difference.

In order to test the influence of the filter design, higher order Butterworth filters are tested. The bandpass filters are then created from the 9th order filters rather than the 7th order. The differences in the EDT and T_{30} with these filters are shown on the right side of Table I. The differences caused by the leakage are smaller when the filters

are sharper, but it is still only the 4 kHz $\Delta EDT_{pb, sin}$ that is below the just noticeable difference.

When choosing and designing filters, their computational cost and stability should be considered. For the present Butterworth filters, the highest possible order for stable filters is 7, if the 125 Hz octave band should be included. Moreover, when filtering to obtain decays in octave bands possible, ringing of the filters in the time domain should also be considered, because it can influence the decays [6]. Ringing in the time domain tends to increase when the filter are sharper in the frequency domain.

5. Concluding remarks

When creating full bandwidth pressure impulse responses from octave band energy responses, the overlaps of the applied bandpass filters influence the decays of the octave bands. The effect can be important when looking at decays, even when the leakage in energy is marginal. If an octave band has a neighbouring band with a slower decay than itself, leakage from the slowly decaying band will make its decay slower when calculated from the full bandwidth impulse response. The shape of the decay curve will furthermore tend to be double-sloped. Even if the construction of the full bandwidth response is done such that there is hardly any overlap between the octave band responses, the overlaps of the filters used for refiltering the full bandwidth response are big enough for spillover between the bands to influence the reverberation times. This indicates that the same will be true when filtering and processing a measured impulse response, which means that the assumption of independent bands in simulations is an approximation and may lead to noticeable errors. Finally, the design of the bandpass filters has an influence on leakage, and sharper filters naturally reduce the effect. But even with sharper filters than required in IEC 61260-1 [8],

the influence on the reverberation time of non-ideal filtering is found to be higher than the JND.

Acknowledgements

The authors are grateful for discussions with James Harte and Søren Laugesen that lead to the findings in this paper.

References

- [1] H. Kuttruff: Auralization of impulse responses modeled on the basis of ray-tracing results. *J. Audio Eng. Soc.* **41** (1993) 876–880.
- [2] C. Lynge, G. Koutsouris, J. Gil: ODEON manual version 13. ODEON, Kgs. Lyngby, 2016.
- [3] D. Schröder: Physically based real-time auralization of interactive virtual environments. Ph.D. thesis, RWTH Aachen, 2011.
- [4] G. Marbjerg, J. Brunskog, C.-H. Jeong, E. Nilsson: Description and validation of a combined phased acoustical radiosity and image source model for predicting sound fields in rooms. *J. Acoust. Soc. Am.* **138** (2015) 1457–1468.
- [5] M. Kob, M. Vorländer: Band filters and short reverberation times. *Acta Acust. united Ac.* **86**, (2000) 350–357.
- [6] F. Jacobsen: A note on acoustic decay measurements. *J. Sound Vib.* **115** (1987) 163–170.
- [7] G. I. Koutsouris, J. Brunskog, C.-H. Jeong, F. Jacobsen: Combination of acoustical radiosity and the image source method. *J. Acoust. Soc. Am.* **133** (2013) 3963–3974.
- [8] IEC 61260-1: Octave-band and fractional-octave-band filters - Part 1: Specifications. European Committee for Electrotechnical Standardization, Brussels, Belgium, 2014.
- [9] ISO standard 9631-1: Attenuation of sound during propagation outdoors - Part 1: Calculation of the absorption of sound by the atmosphere. International Organization for Standardization, Geneva, Switzerland, 1993.
- [10] ISO standard 3382-1: Measurement of room acoustic parameters - Part 1: Performance spaces. International Organization for Standardization, Geneva, Switzerland, 2009.